CCMS-85-06
VPI-E-85-15

VIRGINIA TECH

CENTER FOR COMPOSITE MATERIALS AND STRUCTURES

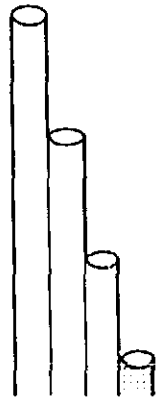

Stresses and Deformations in Cross-Ply Composite Tubes Subjected to a Uniform Temperature Change: Elasticity and Approximate Solutions

M. W. Hyer
David E. Cooper
D. Cohen

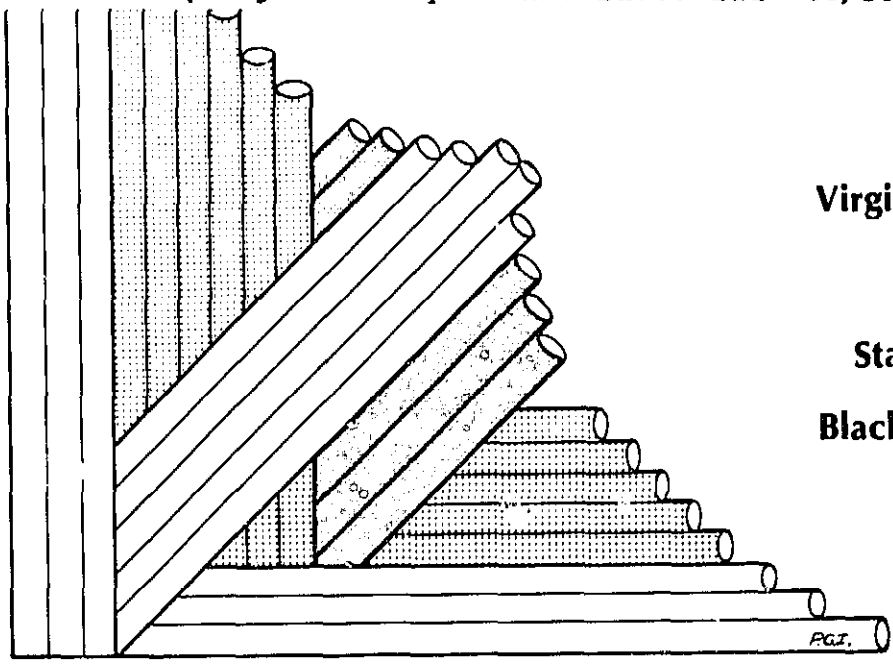

Virginia Polytechnic Institute and State University

Blacksburg, Virginia 24061

College of Engineering
Virginia Polytechnic Institute & State University
Blacksburg, Virginia 24061

CCMS-85-06
VPI-E-85-15

June 1985

Stresses and Deformations in Cross-Ply Composite Tubes Subjected to a Uniform Temperature Change: Elasticity and Approximate Solutions

M. W. Hyer[1]

David E. Cooper[2]

D. Cohen[2]

Department of Engineering Science & Mechanics

Interim Report 51
The NASA - Virginia Tech Composites Program
NASA Cooperative Agreement NAG-1-343

Prepared for: S. S. Tompkins
Applied Materials Branch
National Aeronautics and Space Administration
Langley Research Center
Hampton, VA 23665

[1] Professor, Department of Engineering Science & Mechanics

[2] Graduate Student, Department of Engineering Science & Mechanics

ABSTRACT

The study: (1) Investigates the effects of a uniform temperature change on the stresses and deformations of composite tubes; (2) Determines the accuracy of an approximate solution based on the principle of complementary virtual work. Interest centers on tube response away from the ends and so a planar elasticity approach is used. For the approximate solution a piecewise linear variation of stresses with the radial coordinate is assumed. The results from the approximate solution are compared with the elasticity solution. The stress predictions agree well, particularly peak interlaminar stresses. Suprisingly, the axial deformations also agree well. This despite the fact that the deformations predicted by the approximate solution do not satisfy the interface displacement continuity conditions required by the elasticity solution. The study shows that the axial thermal expansion coefficient of tubes with a specific number of axial and circumferential layers depends on the stacking sequence. This is in contrast to classical lamination theory which predicts the expansion to be independent of the stacking arrangement. As expected, the sign and magnitude of the peak interlaminar stresses depends on stacking sequence. For tubes with a specific number of axial and circumferential layers, thermally-induced interlaminar stresses can be controlled by altering stacking arrangement.

INTRODUCTION

Tubes are efficient structural elements for reacting bending, axial, and torsional loads. In addition, when using fiber-reinforced materials, tubes can be efficiently made using filament winding or one of several other automated techniques. Stiffness, strength, and thermal expansion properties of the tube can be controlled by varying the number of layers of fiber-reinforced material, and by varying the angle of the fibers relative to the axial direction. However, for fiber-reinforced materials like graphite-epoxy, tubes are made by curing the epoxy at an elevated temperature. Typical epoxies cure at 120-175°C (250-350°F) while epoxies made for high temperature operation cure at 290-340°C (550-650°F). Operating a graphite-epoxy tube below the cure temperature of the material can result in high residual stresses. If the stresses are too high, material failure can occur, resulting in a loss of performance of the tube.

Graphite-epoxy tubes are currently being considered as a major building block for large orbiting space structures. Ambient temperatures as low as -156°C (-250°F) can occur in space. To use tubes effectively, understanding their response in these thermal environments is quite important. This paper reports on the calculation of the response of layered tubes to a spatially uniform temperature change. The change represents the difference between the tube fabrication temperature and the temperature of its operating environment. The responses of interest in this paper are the thermally induced stresses and the axial thermal expansion characteristics. The latter response is important for dimensional stability considerations, both during the assembly of large structures, and during operation. Unless dimensional

changes are controlled, orbiting into and out of the earth's shadow can cause problems. Of particular concern is the influence of layering arrangement on stresses and axial expansion.

The tubes considered are of a constant inner and outer diameters. The tubes are made of multiple layers, each layer having properties which represent unidirectional graphite-epoxy. Each layer will be assumed to be homogeneous and either orthotropic or transversely isotropic in a coordinate system aligned with the axis of the tube. In terms of fiber-reinforced material, the study is restricted to what are referred to as cross-ply tubes. A layer is said to be a 0° layer if the stiff, or fiber, direction is axial. A layer is said to be a 90° layer if the fiber direction is circumferential. Stacking sequence notation common to the analysis of layered composite materials will be used. A tube designated as a (90/0/90/0) tube is a cross-ply tube and has four layers. The inner layer and the second layer from the outside have their fibers aligned circumferentially (90°). The outside layer and the second layer from the inside have their fibers aligned axially (0°). A (0/90/0/90) tube would have the fibers in the inner layer oriented axially, etc. Interest centers on the portions of the tube away from the ends. In practice, the end fittings used to connect the tubes together will dictate to a large degree the stress state near the ends. Since these regions on the end of the tube constitute such a small percentage of the total tube length, the overall axial thermal expansion characteristics, for example, could well be determined by the large percentage of the length of the tube away from the ends. Therefore, a generalized plane deformation elasticity solution is used to determine the tube response. The solution assumes that the stresses

are not a function of the axial coordinate of the tube. An elasticity solution, as opposed to a shell-like approach, is used because some tubes being considered for use have mean radius to wall thickness ratios of less than 10. For such a small ratio, through-the-thickness effects have to be accounted for. To account for these effects, a higher-order shell theory could be used. However, an elasticity approach is felt to be more direct.

With a spatially uniform temperature, the problem is assumed to be axisymmetric. Thus, with no dependence of the stresses on the axial coordinate, and using the axisymmetry assumption, the equations governing the tube response reduce to ordinary differential equations. Interesting and useful engineering information is obtained from the solutions. In addition, it is possible to see explicitly how the assumption of transverse isotropy in a layer affects the differential equations governing the behavior of that layer.

Looking beyond the axisymmetric problem, the solution to the axisymmetric problem can serve as a guide for constructing approximate solutions to problems having no closed-form solution. An example of such a problem is the determination of the stresses in a layered tube with temperature-dependent material properties and subjected to a circumferential temperature gradient. Such a condition can exists with a tube in space, with the one side heated by the sun and the other side exposed to the cold of its own shadow. A significant circumferential temperature gradient would exist within the tube. To address such a problem, finite-elements, or some other numerical technique can be used. Here the use of the principle of complementary virtual work, in conjunction with a Ritz approach, is explored. However, here the

circumferential temperature gradient problem is not solved. The axisymmetric problem is resolved in an approximate sense, using simple functional forms for the stresses. The stresses and deformations determined by this approximate approach are compared with the elasticity solutions in order to evaluate the use of this approximate approach for more complicated problems.

The paper begins by deriving the governing equations for the elasticity solution. Key assumptions and their effect on the governing equations are emphasized. The second section presents numerical results based on the elasticity solution. The effect of layering arrangement on the residual stresses and the axial thermal expansion are illustrated. The third section formulates the problem from the point of view of the principle of complementary virtual work and a Ritz approximation to the stress fields. The fourth section presents a comparison between numerical results from the virtual work solution and the elasticity solution. The weak and strong points of the approximate solution are discussed. Though not directly related to the study of tubes, the fifth section presents an interesting sidelight, namely the examination of the residual stresses in a solid cylinder. It is demonstrated that the theory predicts unbounded stresses at the center of the cylinder if the material constants satisfy a certain rather general condition.

DERIVATION OF THE GOVERNING EQUATIONS

Figure 1 shows the coordinate system and nomenclature associated with the layered tube. The inner radius is denoted as r_i, the outer radius r_o, and the radii of the interfaces r_1, r_2, etc. The axial coordinate is x and the displacement in that direction is u. The circumferential coordinate is θ and v denotes circumferential displacement. The radial displacement is w and r the radial coordinate. The usual notation is used to identify the components of stress and strain, i.e., σ_r is the normal stress in the radial direction, $\gamma_{x\theta}$ is the engineering shear strain in the x-θ plane, etc. The temperature of the tube is ΔT above some reference temperature. Here the reference temperature will be the cure temperature of the material and ΔT will be negative. The equations governing a single isolated layer will be derived. The solution to the equations will be expressed in terms of unknown constants of integration and the layer material properties. There will be one such solution for each layer. The constants associated with each layer will be determined by enforcing the stress-free boundary conditions on the inner and outer surface, r_i and r_o, and by enforcing certain interface conditions at r_1, r_2, etc. In addition, because of the planar nature of the solution, certain integrated conditions will be used in the determination of the constants.

Because the problem is axisymmetric and each layer is orthotropic in the x-θ-r coordinate system, the circumferential component of displacement in each layer is zero. Because of axisymmetry, neither of the other two components of displacement depend on the circumferential coordinate. Furthermore, in the portion of the tubes away from the

ends, the radial displacement is a function only of the radial coordinate. With these assumptions, the displacements in each layer take the form:

$$\begin{aligned} u &= u(x,r) \\ v &= 0. \\ w &= w(r) \end{aligned} \tag{1}$$

The strain-displacement relations then simplify to

$$\begin{aligned} &\varepsilon_x = \frac{\partial u}{\partial x} \; ; \; \varepsilon_\theta = \frac{w}{r} \; ; \; \varepsilon_r = \frac{dw}{dr} \\ &\gamma_{x\theta} = 0 \; ; \; \gamma_{xr} = \frac{\partial u}{\partial r} \; ; \; \gamma_{\theta r} = 0, \end{aligned} \tag{2}$$

where the total derivative has been used where possible.

Since each layer is orthotropic, or transversly isotropic, the stress-strain relation for each layer can be expressed in the x-θ-r coordinate system as

$$\begin{Bmatrix} \sigma_x \\ \sigma_\theta \\ \sigma_r \\ \tau_{\theta r} \\ \tau_{xr} \\ \tau_{x\theta} \end{Bmatrix} = \begin{bmatrix} \bar{C}_{11} & \bar{C}_{12} & \bar{C}_{13} & 0 & 0 & 0 \\ \bar{C}_{12} & \bar{C}_{22} & \bar{C}_{23} & 0 & 0 & 0 \\ \bar{C}_{13} & \bar{C}_{23} & \bar{C}_{33} & 0 & 0 & 0 \\ 0 & 0 & 0 & \bar{C}_{44} & 0 & 0 \\ 0 & 0 & 0 & 0 & \bar{C}_{55} & 0 \\ 0 & 0 & 0 & 0 & 0 & \bar{C}_{66} \end{bmatrix} \begin{Bmatrix} \varepsilon_x - \alpha_x \Delta T \\ \varepsilon_\theta - \alpha_\theta \Delta T \\ \varepsilon_r - \alpha_r \Delta T \\ \gamma_{\theta r} \\ \gamma_{xr} \\ \gamma_{x\theta} \end{Bmatrix} . \tag{3}$$

In this coordinate system thermal expansion effects are purely dilatational. The $\bar{C}_{ij}$'s are elastic constants related to the Young's moduli, the Poisson's ratios, and the shear moduli of the material. The α's are the coefficients of thermal expansion. Here all properties will be assumed to be temperature-independent but the methodology is

valid for the temperature-dependent situation. The material constants are different for each layer and Appendix 1 gives expressions for the $\bar{C}_{ij}$ in terms of the more familiar engineering constants (E_1, E_2, ..., ν_1, ..., α_1, ...) in the principal material system.

By eq. 2 and the stress-strain relation,

$$\tau_{x\theta} = 0 = \tau_{\theta r} \quad . \tag{4}$$

Since all stresses are independent of x and θ, all the strains are also. Using this fact, along with the definitions of ε_r and ε_θ from eq. 2, four of the six compatibility equations are automatically satisfied. The two that are not reduce to

$$\begin{aligned} \frac{d^2\varepsilon_x}{dr^2} &= 0 \\ \frac{1}{r}\frac{d\varepsilon_x}{dr} &= 0 \quad . \end{aligned} \tag{5}$$

Integrating the first of these leads to

$$\varepsilon_x(r) = Ar + B \quad , \tag{6}$$

A and B being constants. The second equation requires A to be zero. Redefining B to be ε^o,

$$\varepsilon_x(r) = \varepsilon^o \tag{7}$$

and it is seen that the axial strain in a layer is not a function of any of the coordinate variables.

Likewise, with the assumptions of the independence of the stresses of x and θ, and using eq. 4, the equilibrium equations simplify to

$$\frac{d\sigma_r}{dr} + \frac{\sigma_r - \sigma_\theta}{r} = 0$$

$$\frac{d\tau_{xr}}{dr} + \frac{\tau_{xr}}{r} = 0, \tag{8}$$

the third one being automatically satisfied. Integrating the second equation results in

$$\tau_{xr} = \frac{C}{r} , \tag{9}$$

C being a constant.

The functional form of u(x,r) can be found from the above results. Using eq. 7, the first strain-displacement relation (eq. 2) integrates to

$$u(x,r) = \varepsilon^o x + f(r) , \tag{10}$$

f(r) being an arbitrary function of r. From eqs. 2, 3, and 9,

$$\gamma_{xr} = \frac{du}{dr} = \frac{df}{dr} = \frac{\tau_{xr}}{\bar{C}_{55}} = \frac{C}{\bar{C}_{55}} \frac{1}{r} \tag{11}$$

or

$$f(r) = \frac{C}{\bar{C}_{55}} \ln r + D, \tag{12}$$

D being a constant. With this result

$$u(x,r) = \varepsilon^o x + \frac{C}{\bar{C}_{55}} \ln r + D. \tag{13}$$

By writing the stresses in terms of the displacements, the first equilibrium equation leads to a differential equation for w(r), namely

$$\bar{C}_{33}\left(\frac{d^2w}{dr^2} + \frac{1}{r}\frac{dw}{dr}\right) - \bar{C}_{22}\frac{w}{r^2} = \frac{1}{r}(\bar{C}_{12} - \bar{C}_{13})\varepsilon^o + \frac{\bar{\Sigma}}{r} , \tag{14}$$

where

$$\bar{\Sigma} = (\bar{C}_{13} - \bar{C}_{12})\alpha_x + (\bar{C}_{23} - \bar{C}_{22})\alpha_\theta + (\bar{C}_{33} - \bar{C}_{23})\alpha_r)\Delta T \quad . \quad (15)$$

With the solution to u(x,r) available and by solving for w(r), the complete solution is available for application to either a single-layer problem or to a multiple-layer problem.

SOLUTION FOR w(r)

Equation 14 has a solution of the form

$$w(r) = A_1 r^{\lambda} + A_2 r^{-\lambda} + \frac{(\bar{C}_{12} - \bar{C}_{13})}{(\bar{C}_{33} - \bar{C}_{22})} \varepsilon^o r + \bar{\Sigma}\, r \quad (16)$$

with

$$\lambda = \sqrt{\frac{\bar{C}_{22}}{\bar{C}_{33}}} \quad (17)$$

Many times it is assumed that a layer of fiber-reinforced material is transversely isotropic in the plane perpendicular to the fibers. In the nomenclature of Appendix 1, and in the nomenclature common to fiber-reinforced materials, this is the 2-3 plane. While isotropy in that plane may not be exactly satisfied, for lack of complete material property data, transverse isotropy is often assumed. Referring to Appendix 1 for nomenclature, the assumption of transverse isotropy implies

$$E_3 = E_2;\ \nu_{13} = \nu_{12};\ G_{23} = \frac{E_2}{2(1 - \nu_{23})}\ ;\ \alpha_2 = \alpha_3 \quad (18)$$

In this problem the assumption influences the equation governing the behavior of a 0° layer. For a transversely isotropic 0° layer,

$$\bar{C}_{33} = \bar{C}_{22}\ ;\ \bar{C}_{13} = \bar{C}_{12},\ \alpha_r = \alpha_\theta\ , \quad (19)$$

and the equation for w(r), eq. 14, becomes homogeneous and not dependent

on material properties. The equation becomes

$$\frac{d^2w}{dr^2} + \frac{1}{r}\frac{dw}{dr} - \frac{w}{r^2} = 0 \tag{20}$$

and has solution

$$w(r) = A_1 r + \frac{A_2}{r} \tag{21}$$

To determine the constants A_1, A_2, C, D and ε^o, boundary, interface, and an integral condition must be applied.

BOUNDARY CONDITIONS

Single Layer

The conditions for a single layer are that tractions vanish at the inner and outer radii, namely,

$$\sigma_r(r_i) = 0;\ \sigma_r(r_o) = 0;\ \tau_{xr}(r_i) = 0;\ \tau_{xr}(r_o) = 0$$
$$\tau_{\theta r}(r_i) = 0;\quad \tau_{\theta r}(r_o) = 0 \tag{22a-f}$$

and that the net axial force acting on the cross-section of the layer is zero. This axial force condition can be expressed as

$$\int_A \sigma_x r\,d\theta\,dr = 0\ , \tag{23}$$

where A is the cross-sectional annular area of the layer. The integral can be written more specifically as

$$2\pi \int_{r_i}^{r_o} \sigma_x(r) r\ dr = 0. \tag{24}$$

Other resultant equations, such as the net cross-sectional moment and the net torsional moment being zero, can be written for the cross-section. However, all except eq. 23 are automatically satisfied. As a final condition, rigid body displacements of the layer must be

suppressed.

By eq. 4, eqs. 22e and f are automatically satisfied. Application of eqs. 22c and d requires C of eqs. 9 and 13 to be zero. Suppressing rigid body axial motion forces D of eq. 13 to be zero. As a result

$$u(x,r) = \varepsilon^{o}x. \tag{25}$$

Applying eqs. 22a and b, and eq. 24 leads to three equations for A1, A2, and ε^{o}. With these coefficients known, the stresses and displacements in a single layer can be determined.

Multiple Layers

For multiple layers, the solutions for $\tau_{xr}(r)$, u(x,r), and w(r) in eqs. 9, 13 and 16 require a different set of constants for each layer. Because the material constants for each layer can be different, the value of λ will be different for each layer. For the kth layer,

$$\tau_{xr}^{(k)} = \frac{C^{(k)}}{r}, \tag{26}$$

$$u^{(k)}(x,r) = \varepsilon^{o(k)}x + \frac{C^{(k)}}{\bar{C}_{55}^{(k)}} \ln r + D^{(k)}, \tag{27}$$

and

$$w^{(k)}(r) = A_1^{(k)}r^{\lambda^{(k)}} + A_2^{(k)}r^{-\lambda^{(k)}} + \frac{(\bar{C}_{12}^{(k)} - \bar{C}_{13}^{(k)})}{(\bar{C}_{33}^{(k)} - \bar{C}_{22}^{(k)})} \varepsilon^{o^{(k)}} r + \bar{\Sigma}^{(k)}r,$$

where

$$\bar{\Sigma}^{(k)} = ((\bar{C}_{13}^{(k)} - \bar{C}_{12}^{(k)})\alpha_x^{(k)} + (\bar{C}_{23}^{(k)} - \bar{C}_{22}^{(k)})\alpha_\theta^{(k)} + (\bar{C}_{33}^{(k)} - \bar{C}_{23}^{(k)})\alpha_r^{(k)})\Delta T,$$

and

$$\lambda^{(k)} = \sqrt{\frac{\bar{C}_{22}^{(k)}}{\bar{C}_{33}^{(k)}}}. \tag{29}$$

If the layer is transversely isotropic,

$$w^{(k)}(r) = A_1^{(k)} r + \frac{A_2^{(k)}}{r} \quad . \tag{30}$$

For N layers, there are N ϵ^o's, N C's, N D's, N A1 and N A2's, or 5N unknown constants. These constants are determined by satisfying the traction-free conditions on the inner and outer radii, satisfying continuity of tractions at each interface, satisfying continuity of displacements at each interface, suppressing rigid body motion, and by applying an integrated condition on the cross-sectional area. These are explained below.

Since layer 1 is the inner layer and layer N is the outer layer, the traction-free conditions at the inner and outer radii are

$$\sigma_r^{(1)}(r_i) = 0 \; ; \; \tau_{xr}^{(1)}(r_i) = 0 \; ; \; \tau_{\theta r}^{(1)}(r_i) = 0 \tag{31a-c}$$

$$\sigma_r^{(N)}(r_o) = 0 \; ; \; \tau_{xr}^{(N)}(r_o) = 0 \; ; \; \tau_{\theta r}^{(N)}(r_o) = 0. \tag{31d-f}$$

By eq. 4, eqs. 31c and f are automatically satisfied. Equations 31b and e lead to, from eq. 26,

$$C^{(1)} = C^{(N)} = 0. \tag{32}$$

Continuity of the interface tractions can be expressed as

$$\sigma_r^{(k)}(r_k) = \sigma_r^{(k+1)}(r_k) \; ; \; \tau_{xr}^{(k)}(r_k) = \tau_{xr}^{(k+1)}(r_k) \; ;$$

$$\tau_{\theta r}^{(k)}(r_k) = \tau_{\theta r}^{(k+1)}(r_k) \quad , \quad k = 1,2,\ldots,N-1. \tag{33a-c}$$

Again by eq. 4, eq. 33c is automatically satisfed. Equation 33b, along with eq. 32, leads to the conclusion that

$$C^{(k)} = 0 \quad , \quad k = 1,N. \tag{34}$$

More will be said of eq. 33a shortly.

Continuity of the interface displacement can be written as

$$u^{(k)}(r_k,x) = u^{(k+1)}(r_k,x) \; ; \; v^{(k)}(r_k) = v^{(k+1)}(r_k) \; ;$$

$$w^{(k)}(r_k) = w^{(k+1)}(r_k) \quad , \quad k = 1,2,\ldots,N-1. \tag{35}$$

Obviously since $v = 0$ in all layers, continuity of the circumferential displacements is automatically satisfied. Substituting from eq. 27, and using eq. 34, eq. 35a results in

$$\varepsilon^{o(k)}x + D^{(k)} = \varepsilon^{o(k+1)}x + D^{(k+1)} \quad , \quad k = 1,2,\ldots,N-1. \tag{36}$$

This equation leads to the conclusion that the constant axial strain for each layer is the same for all layers and so the tube-as-a-whole has strain ε^o. This strain is given by

$$\varepsilon^{o(k)} = \varepsilon^o \quad , \quad k = 1,N \; . \tag{37}$$

Also from eq. 36, all $D^{(k)}$ must be equal and, if axial rigid body motion is eliminated,

$$D^{(k)} = 0 \quad , \quad k = 1,N \; . \tag{38}$$

At this point

$$u^{(k)}(r,x) = \varepsilon^o x \tag{39}$$

and

$$w^{(k)}(r) = A_1^{(k)} r^{\lambda^{(k)}} + A_2^{(k)} r^{-\lambda^{(k)}} + \left(\frac{\bar{C}_{12}^{(k)} - \bar{C}_{13}^{(k)}}{\bar{C}_{33}^{(k)} - \bar{C}_{22}^{(k)}}\right)\varepsilon^o r + \bar{\Sigma}^{(k)} r \tag{40}$$

or

$$w^{(k)}(r) = A_1^{(k)} r + \frac{A_2^{(k)}}{r} \; . \tag{41}$$

These expressions for u and w involve N A_1's, N A_2's, and ε^o, or 2N + 1

unknowns. The first and fourth of eq. 31, the first of eq. 33, and the third of eq. 35 provide 2N equations. The remaining necessary equation is determined by the integral condition that there is no net axial force acting on the cross section of the tube, i.e.,

$$\int_A \sigma_x r d\theta dr, \tag{42}$$

where now A is the annular area of all N layers. Specifically this condition is written as

$$2\pi \sum_{k=1}^{N} \int_{r_{k-1}}^{r_k} \sigma_x^{(k)} r dr = 0 . \tag{43}$$

The complete solution for the displacements, and hence the stresses, for the N layers is now available. This whole process can be easily automated for an arbitrary number of layers, each with arbitrary but orthotropic or transversely isotropic material properties.

NUMERICAL RESULTS

To illustrate some of the thermal effects that occur in layered composite tubes, the numerical results for several specific problems will be presented. Table 1 lists the material and geometric properties used in these numerical examples.

Effect of Stacking Sequence on Residual Stresses

Figures 2 and 3 illustrate the residual axial, circumferential (hoop), and radial stresses in two four-layer graphite-epoxy tubes. The tube in fig. 2 has a stacking sequence of (0/90/0/90) while the tube of fig. 3 has a stacking sequence of (90/0/90/0). Each tube is at a temperature 280°C (500° F) lower than its curing temperature. As far as axial stiffness is concerned, these two tubes are practically identical,

as are other combinations of two 0° layers and two 90° layers. (Axial stiffness is an important design parameter in many space structures.) In the figures the stresses are illustrated as a function of the nondimensional radius ρ, $\rho = (r - r_i) / (r_o - r_i)$.

By examining figs. 2 and 3 it can be seen that for both tube configurations there are high tensile stresses perpendicular to the fiber direction. Also, there are high compressive stresses in the fiber direction. The magnitude of the tensile stresses are such that the brittle epoxy could easily crack. These high stresses could be expected and predicted to some degree of accuracy without resorting to elasticity theory. However, it has been found for these particular cross-ply tubes, the less refined theories, e.g., classical lamination theory, underpredict the compressive stresses in the hoop direction. In addition, figs. 2 and 3 show an interesting effect concerning the radial stresses that can only be predicted using the more refined theory. Figure 2 shows that for the (0/90/0/90) tube the interface between the outer 0° and 90° layers experiences a tensile radial stress. The value of the tensile stress is not high compared to the axial and circumferential stress components. However, the peak tensile stress occurs at an interface between layers, a region that can be weaker in tension than the other portions of the tube. Figure 3 shows that by interchanging layer order, the interface with the peak stress now experiences a compressive stress and the peak tensile stress, which is now at another interface, is considerably less.

Effect of Stacking Sequence on the Coefficient of Thermal Expansion

As the temperature of the tube is reduced below its cure temperature, the thermal expansion effects, coupled with the elastic

properties, will produce a change in length of the tube. The quantity ε^o is a measure of this axial deformation. Recall that ε^o is the same for all layers. The quantity formed by dividing ε^o by ΔT is the axial coefficient of thermal expansion (CTE) of the tube. For dimensional stability studies, this expansion coefficient is of great interest. As will now be demonstrated, stacking sequence influences this quantity to some degree.

If all combinations of four-layer tubes with the fibers in two layers being axial and the fibers in the two other layers being circumferential are considered, six different stacking sequences are possible. Table 2 shows the axial CTE's of these six combinations. Suprisingly enough, the coefficients vary by 7% among the six tubes. While a 7% variation may seem low, there have been efforts to construct tubes with a specific axial CTE. It would seem that stacking arrangement, as well as fiber orientation, could be used to help achieve this.

Further Examples

To provide motivation for the next portion of the paper, and to provide other examples of residual effects, a $(90/0_6/90)$ tube is considered. Such a tube is a prime candidate for structural applications. This tube has a high axial stiffness due to 80% of the fibers being in the axial direction. The circumferential layers are referred to as skins while the six axial layers are referred to as the core. The skins serve to keep the axial layers together. However, these circumferential layers contribute significantly to the thermal stress state.

Figure 4 shows the three components of thermally induced stress for this skin/core tube. In both the skin and the core the fibers are in

compression. Due to the high axial stresses in the skins, the skins probably will exhibit circumferential cracks. This does not degrade their function of holding the core together. The core itself could well have cracks in it also. The cracks would be radial, running the length of the tube. There is a tensile peak in the radial stress between the outer skin and the core. The radial stress between the inner skin and the core is compressive.

If the effects of temperature-dependent material properties are important in a particular instance, the preceeding analysis can be used. Temperature dependence of the $\overline{Q}_{ij}$'s and the α's does not affect any of the derivation. However, as mentioned in the INTRODUCTION, the effects of circumferential temperature gradients on the stresses could be of interest. If the material properties are assumed to be independent of temperature, closed-form solutions may be possible, depending on the functional form of the gradient. However, if temperature-dependent material properties are to be included with a circumferential gradient, closed-form solutions are probably not possible, except for some special cases. In general, an approximate method would have to be used to determine the stresses. The next section explores the use of the principle of complementary virtual work in conjunction with a Ritz approximation to the stress fields to study thermal stresses in layered tubes. Only the uniform temperature case just considered will be studied. However, comparisons of the complementary virtual work approach with the elasticity solution will serve as a measure of the accuracy of the approximate approach.

APPROXIMATE METHOD BASED ON COMPLEMENTARY VIRTUAL WORK

For the problem here, if the volume V is considered as the volume

for all N layers, and the surface S is considered as the inner surface plus the outer surface of the tube, the principle of complementary virtual work can be written as

$$\int_V (\varepsilon_x \delta\sigma_x + \varepsilon_\theta \delta\sigma_\theta + \varepsilon_r \delta\sigma_r + \gamma_{\theta r}\delta\tau_{\theta r} + \gamma_{xr}\delta\tau_{xr} + \gamma_{x\theta}\delta\tau_{x\theta})dV$$

$$+ \int_S (u\delta T_x + v\delta T_\theta + w\delta T_r)dS = 0 \quad . \tag{44}$$

For this problem the tractions on the surface, T_x, T_θ, T_r, are known, specifically they are zero. Therefore the surface integral is not involved. Implicit in the above equation is the fact that the stresses being varied must satisfy the equilibrium equations and the traction boundary and interface continuity conditions.

When using the complementary principle it is more convenient to invert the stress-strain relation of eq. 3 and write (see Appendix 1)

$$\begin{Bmatrix} \varepsilon_x - \alpha_x\Delta T \\ \varepsilon_\theta - \alpha_\theta\Delta T \\ \varepsilon_r - \alpha_r\Delta T \\ \gamma_{\theta r} \\ \gamma_{xr} \\ \gamma_{x\theta} \end{Bmatrix} = \begin{bmatrix} \bar{S}_{11} & \bar{S}_{12} & \bar{S}_{13} & 0 & 0 & 0 \\ \bar{S}_{12} & \bar{S}_{22} & \bar{S}_{23} & 0 & 0 & 0 \\ \bar{S}_{13} & \bar{S}_{23} & \bar{S}_{33} & 0 & 0 & 0 \\ 0 & 0 & 0 & \bar{S}_{44} & 0 & 0 \\ 0 & 0 & 0 & 0 & \bar{S}_{55} & 0 \\ 0 & 0 & 0 & 0 & 0 & S_{66} \end{bmatrix} \begin{Bmatrix} \sigma_x \\ \sigma_\theta \\ \sigma_r \\ \tau_{\theta r} \\ \tau_{xr} \\ \tau_{x\theta} \end{Bmatrix} . \tag{45}$$

Approximate solutions to the thermal stress state can be obtained from eq. 44 by assuming that the stresses can be expressed in terms of specific functional forms and unknown coefficients. Explicitly integrating the volume integral results in Euler equations, in the form of linear algebraic equations, which can be solved for the unknown coefficients. The nature of the stresses illustrated in figs. 2-4

provides a strong motivation for assuming a simple linear variation of stresses within each layer. If circumferential temperature gradients were involved it would make sense to assume the stresses could be approximated by the product of function of θ and linear function of r. Thus for an N-layer tube, the stresses are assumed to be of the form

$$\begin{aligned} \sigma_x^{(k)} &= c_o^{(k)} + c_1^{(k)} r \\ \sigma_\theta^{(k)} &= b_o^{(k)} + b_1^{(k)} r \qquad k = 1,N \ , \\ \sigma_r^{(k)} &= a_o^{(k)} + a_1^{(k)} r \end{aligned} \tag{46}$$

all other stresses being zero. The superscript denotes layer number and $a_o^{(k)},\ldots,c_1^{(k)}$ are to-be-determined constants. For a N-layer tube there are 6N constants. However, to use these in the virtual work statement the assumed stresses must satisfy the equations of equilibrium and the traction boundary conditions. In addition, for this problem there are two further conditions. The first one is that σ_r must be continuous at the interfaces between layers. The second one is that the axial stresses in the layers must be such that the net axial force is zero.

To satisfy the equilibrium equations, eq. 8,

$$a_o^{(k)} = b_o^{(k)} \text{ and } 2a_1^{(k)} = b_1^{(k)}, \quad k = 1,N \ . \tag{47}$$

Since the inner and outer layer (k = 1 and N) are traction free at $r = r_i$ and $r = r_o$, respectively, applying eqs. 31a and d to eq. 46 leads to

$$\begin{aligned} a_o^{(1)} + a_1^{(1)} r_i &= 0 \\ a_o^{(N)} + a_1^{(N)} r_o &= 0 \ . \end{aligned} \tag{48}$$

Because σ_r is continuous at the interface between the kth and (k + 1)st

layers,

$$a_o^{(k)} + a_1^{(k)} r_k = a_o^{(k+1)} + a_1^{(k+1)} r_k \quad , \; k = 1, N-1 \; . \tag{49}$$

The remaining condition on the approximate stresses is the integrated condition on the cross-section, eq. 42. This leads to

$$2\pi \{ \int_{r_i}^{r_1} (c_o^{(1)} + c_1^{(1)} r) r dr + \sum_{k=2}^{N} \int_{r_k}^{r_{k-1}} (c_o^{(k)} + c_1^{(k)} r) r dr + \int_{r_{N-1}}^{r_o} (c_o^{(N)} + c_1^{(N)} r) r dr \} = 0 \tag{50}$$

For a two-layer tube, for example, the stresses that satisfy the above conditions are given by

layer 1

$$\begin{aligned} \sigma_x &= c_1^{(1)} + c_1^{(1)} r \\ \sigma_\theta &= a_1^{(1)} (2r - r_i) \\ \sigma_r &= a_1^{(1)} (r - r_i) \end{aligned} \tag{51}$$

layer 2

$$\begin{aligned} \sigma_x &= c_1^{(2)} (r - \beta_3) - \beta_1 c_1^{(1)} - \beta_2 c_o^{(1)} \\ \sigma_\theta &= a_1^{(1)} \left(\frac{r_1 - r_i}{r_1 - r_o} \right) (2r - r_o) \\ \sigma_r &= a_1^{(1)} \left(\frac{r_1 - r_i}{r_1 - r_o} \right) (r - r_i) \end{aligned} \tag{52}$$

The quantities β_1, β_2, and β_3 are known constants involving the tube geometry. They are defined in Appendix 2. There are four constants, $a_1^{(1)}$, $c_o^{(1)}$, $c_1^{(1)}$, $c_1^{(2)}$, that determine the stress state. For a three layer tube there are seven constants.

Substituting the stresses into the strains and the strains into eq. 44, and also substituting the first variations of the stresses into eq. 44, integration of eq. 44 leads to an equation of the form

$$f_1(a_1^{(1)}, c_o^{(1)}, c_1^{(1)}, c_1^{(2)})\delta a_1^{(1)} + f_2(a_1^{(1)}, c_o^{(1)}, c_1^{(1)}, c_1^{(2)})\delta c_o^{(1)} + f_3(a_1^{(1)}, c_o^{(1)}, c_1^{(1)}, c_1^{(2)})\delta c_1^{(1)} + f_4(a_1^{(1)}, c_o^{(1)}, c_1^{(1)}, c_1^{(2)})\delta c_1^{(2)} = 0. \tag{53}$$

The equations

$$f_i = 0 \quad , \quad i = 1,4 \tag{54}$$

lead to solutions for $a_1^{(1)}$, $c_o^{(1)}$, $c_1^{(1)}$ and $c_1^{(2)}$.

NUMERICAL EXAMPLES USING APPROXIMATE METHOD

Figures 5-7 show examples of the predictions of the approximate method. The exact elasticity solution is included in each example - as a comparison. The examples depict situations designed to illustrate the level of accuracy of the approximate method rather than to illustrate results of engineering significance.

Figure 5 shows the three components of stress for a $(0_3/90)$ tube. Though this really is a four-layer tube, it is modeled as a two-layer tube, the 0° layer being three times thicker than the 90° layer. Despite this lumping of the layers, the comparison between the approximate approach and the exact solution is quite good. The correlation seen here is about as good as has been observed in these studies. As has been seen with the elasticity solution, the peak radial stresses generally occur at the interface between layers of dissimilar orientation. It has been found that the approximate method will accurately

predict the peak value of radial stress at the interfaces even though at other locations the predictions for this same stress are not as good.

Figure 6 shows the results for a $(90_3/0)$ tube. Again the three 90° layers are lumped together and are represented as one layer. While the axial stress and the peak radial interface stress are accurately predicted, the circumferential stresses in the 90° layers are not accurately predicted. Similarly, the predictions of the radial stress in the 90° layers is poor. The correlation seen here is about as poor as observed in this study. It has been found in these studies that the thicker the grouping of layers with circumferential fibers, the less accurate is the approximate method. The principle of complementary virtual work with linear stress approximations tends to underpredict the peak circumferential stress. For these residual stress states, with a negative ΔT, the inaccurate circumferential stresses represent compression in the fiber direction. Since compression in the fiber direction is not a concern in these tubes, this error, at least in this study, is tolerable. Of course, when using the approximate method, a further discretization of the grouped layers helps improve the prediction. Figure 7 shows the effects of splitting the one three-layer grouping in the $(90_3/0)$ in half and representing it with two layers. The tube is then represented by three layers. The principle of complementary virtual work uses the extra degrees of freedom quite efficiently. With just this refinement it is easy to predict the results of addition discretization of the group of 90°'s.

Finally, fig. 8 shows the comparison between the approximate method and the theory of elasticity for a tube of engineering interest, the $(90/0_6/90)$ tube examined before. It is clear that the fairly crude

approximation to the stress fields provides a good estimate of the stress state. It is expected that when a circumferential temperature gradient and temperature-dependent material properties are considered for this type of tube, the linear approximation to the stress fields should be sufficiently accurate for parameter studies.

DEFORMATIONS PREDICTED USING THE PRINCIPLE OF COMPLEMENTARY VIRTUAL WORK

While the principle of complementary virtual work is ideal if concern is solely with the stress state, it is of interest to study the deformations predicted by the principle and compare the results with the predictions of elasticity.

By using the assumed stress fields in the stress-strain relation of eq. 45, the strains for the kth layer can be written in the form

$$\begin{aligned} \varepsilon_x^{(k)} &= A^{(k)} + \alpha_x^{(k)}\Delta T + B^{(k)}r \\ \varepsilon_\theta^{(k)} &= C^{(k)} + \alpha_\theta^{(k)}\Delta T + D^{(k)}r \\ \varepsilon_r^{(k)} &= E^{(k)} + \alpha_r^{(k)}\Delta T + F^{(k)}r \end{aligned} \tag{55}$$

There are no shear strains. In the above the quantities $A^{(k)},\ldots,F^{(k)}$ are functions of the layer compliance, $\bar{S}_{ij}$, and the constants in the assumed form of the stresses, $a_o^{(k)}$, ..., $c_1^{(k)}$, for that layer. Not surprisingly, the above form of the strains do not satisfy the compatibility equations. Therefore any predictions regarding deformations must be viewed with caution. However, it is instructive to examine the predicted axial CTE for several of the cases shown in Table 1. Table 3 indicates the values of the axial CTE's for four of the six tubes of Table 1. Only these four were examined because the approximate analysis was limited to tubes with a maximum of three layers. The

term α_x in Table 3 is the free thermal expansion of each particular layer in the axial direction. They are taken from Table 1. The term labeled 'approximate axial CTE' is the quantity $((A/\Delta T) + \alpha_x)$ and from eq. 55 is the portion of $\epsilon_x^{(k)}$ that does not vary with r. The terms $A/\Delta T$ and $B/\Delta T$ represent the effect of the other layers on the free axial expansion of the particular layer. It is clear that the $B/\Delta T$ term contributes very little to $\epsilon_x^{(k)}$. This might be expected since the elasticity solution predicts $\epsilon_x^{(k)}$ to be independent of r. The fourth column of Table 3 is the axial CTE predicted by the theory of elasticity. (Recall, the theory of elasticity predicts that the axial CTE is the same in all layers.) The agreement between theory and the approximate method is quite good. With the breakdown in Table 3 it is interesting to see how $A/\Delta T$ contributes to the overall axial expansion of a particular layer. For example, if α_x is large, $A/\Delta T$ is negative. This means that the other layers must restrain the large free thermal expansion value so the deformation of the layer is, to some degree, compatible with the deformations of the other layers. Since compatibility is not satisfied, and since the approximate solution makes no explicit statements regarding continuity of interface displacements, the results of Table 3 are remarkable.

THERMAL STRESSES IN A SOLID CYLINDER

As a final note, consider the case of a solid and unlayered orthotropic cylinder. Equations 9, 13, and 16 govern the behavior of the cylinder. In this case there is no inner radius at which to apply the boundary conditions. Rather, statements must be made regarding boundedness at the origin, as well as satisfying the boundary conditions on the outer surface, and the integral condition. Specifically,

$$\sigma_r(r_o) = 0 \; ; \; \tau_{xr}(r_o) = 0, \tag{56}$$

and $w(r)$ and $u(x,r)$ remain bounded as $r \to 0$,

$$\text{i.e., } w(r),\ u(x,r) < \infty,\ r \to 0. \tag{57}$$

Also,

$$\int_A \sigma_x r dr d\theta. \tag{58}$$

Since $\lambda > 0$, the boundedness condition on $w(r)$ of eq. 16 requires

$$A_2 = 0 \ . \tag{59}$$

The condition on the shear stress τ_{xr} at $r = r_o$ and the suppression of axial rigid body translation requires

$$C = 0 \text{ (eq. 9)},$$

$$D = 0 \text{ (eq. 13)}. \tag{60}$$

The constants A_1 and ε^o can be determined from the condition of the vanishing of the normal stress at $r = r_o$ and the integral condition. In general, neither A_1 nor ε^o are zero.

For the solid cylinder the nonzero stresses are proportional to $r^{\lambda-1}$. If $\bar{C}_{22} > \bar{C}_{33}$, then λ is greater than unity. At $r = 0$ all three components of stress are zero. On the other hand, if $C_{22} < C_{33}$, then λ is less than unity and the stresses are unbounded at $r = 0$. The case $\bar{C}_{22} < \bar{C}_{33}$ corresponds to the situation when the fibers in the cylinder are oriented radially. It may be difficult to manufacture such a cylinder and have the material properties remain constant with radius. Nonetheless, for this case the tube would be much stiffer in the radial direction than in the circumferential direction. Figure 9 shows the three components of stress for the case of using the material properties of Table 1 and assuming the fibers are oriented radially. The value of λ is 0.298. It should be mentioned that the value of λ is a material property and is independent of the fact that the problem is a

thermal stress problem. The stresses are proportional to $r^{\lambda-1}$ near the origin for the case of mechanical loads, e.g., an axial load, being applied to the cylinder.

While the infinite stress is physically impossible, the coefficient of the infinite stress is of interest. The coefficient is an indication of the severity of the stress gradient near the centerline of the cylinder. Unlike the numerical value of λ, this coefficient is a function of whether or not the cylinder is loaded thermally or mechanically. The coefficient also depends on the radius of the cylinder. In fracture mechanics this coefficient is related to the stress intensity factor. Table 4 presents the stress intensity factors for the three nonzero components of stress. It is clear from the table that the radial stress is the most intense as the centerline of the tube is approached. Since the three intensity factors are positive, cooling the tube results in high compressive stresses near the centerline. This situation is more favorable than having high tensile stresses, particularly in the matrix direction.

CONCLUSIONS

From the results presented, it can be concluded that for cross-ply composite tubes cured at an elevated temperature, residual thermal stresses can be of significant magnitude. The peak stresses, as well as the axial CTE, are influenced by the stacking arrangement. It appears that the principle of complementary virtual work, in conjunction with a Ritz approach, can be used to estimate the thermally-induced stresses. The approach also can be used to predict the axial deformations with a remarkable degree of accuracy. This, despite the lack of the approximate solutions satisfying the compatibility equations. When

considering approximate solutions to thermal stress problems it would seem that stress-based approaches, such as the principle of complementary virtual work, are preferrable over displacement-based approaches. For thermal stress problems, displacements need not be considered and so there is no need to approximate variables which must be differentiated to determine the real quantity of interest. Finally, in the idealization of linear elasticity, it appears solid orthotropic cylinders can experience high stress gradiants at their centers.

ACKNOWLEDGEMENTS

The work reported on here was supported by the NASA - Virginia Tech Composites Program, NASA Coorporative Agreement NAG-1-343. S. S. Tompkins of the NASA-Langley Research Center monitored the work.

TABLE 1

Material and Geometric Properties

E_1 = 146.8 GPa; E_2 = 9.929 GPa; E_3 = 9.101 GPa psi

ν_{12} = 0.3; ν_{13} = 0.3; ν_{23} = 0.49

$\alpha_1 = -0.0774 \times 10^{-6}/°C$; $\alpha_2 = 33.66 \times 10^{-6}/°C = \alpha_3$

r_i = 6.35 mm, layer thickness = 0.127mm

TABLE 2

Axial Coefficients of Thermal Expansion
For Cross-Ply Tubes

Tube	axial CTE (per °C)
$(90_2/0_2)$	2.468×10^{-6}
(90/0/90/0)	2.538×10^{-6}
$(0/90_2/0)$	2.601×10^{-6}
$(90/0_2/90)$	2.612×10^{-6}
(0/90/0/90)	2.675×10^{-6}
$(0_2/90_2)$	2.740×10^{-6}

TABLE 3

Axial Coefficients of Thermal Expansion
for Cross-Ply Tubes: Approximate Approach

Tube	Layer	α_x (per °C)	$\frac{A}{\Delta T}$ (per °C)	$\frac{B}{\Delta T}$ (per °C)	approximate axial CTE (per °C)	exact axial CTE (per °C)
$(90_2/0_2)$	90_2	33.66×10^{-6}	-31.19×10^{-6}	-11.81×10^{-17}	2.47×10^{-6}	2.47×10^{-6}
	0_2	-0.077×10^{-6}	2.54×10^{-6}	-17.4×10^{-18}	2.47×10^{-6}	2.47×10^{-6}
$(0/90_2/0)$	0	-0.077×10^{-6}	2.68×10^{-6}	-2.22×10^{-20}	2.60×10^{-6}	2.60×10^{-6}
	90_2	33.66×10^{-6}	-31.06×10^{-6}	-4.22×10^{-16}	2.60×10^{-6}	2.60×10^{-6}
	0	-0.077×10^{-6}	2.68×10^{-6}	-1.89×10^{-15}	2.60×10^{-6}	2.60×10^{-6}
$(90/0_2/90)$	90	33.66×10^{-6}	-31.05×10^{-6}	-3.75×10^{-20}	2.61×10^{-6}	2.61×10^{-6}
	0_2	-0.077×10^{-6}	2.69×10^{-6}	-4.40×10^{-16}	2.61×10^{-6}	2.61×10^{-6}
	90	33.66×10^{-6}	-31.05×10^{-6}	5.09×10^{-16}	2.61×10^{-6}	2.61×10^{-6}
$(0_2/90_2)$	0_2	-0.077×10^{-6}	2.82×10^{-6}	7.06×10^{-16}	2.74×10^{-6}	2.74×10^{-6}
	90_2	33.66×10^{-6}	-30.92×10^{-6}	5.91×10^{-17}	2.74×10^{-6}	2.74×10^{-6}

TABLE 4

Stress Intensity Factors For Solid Cylinder
($\bar{C}_{22} < \bar{C}_{33}$)

Stress Component	Coefficient of $r^{\lambda-1}$ *
σ_x	0.0848
σ_θ	0.1303
σ_r	0.4366

* units are such that stress is in MPa/°C increase in temperature above the reference temperature.

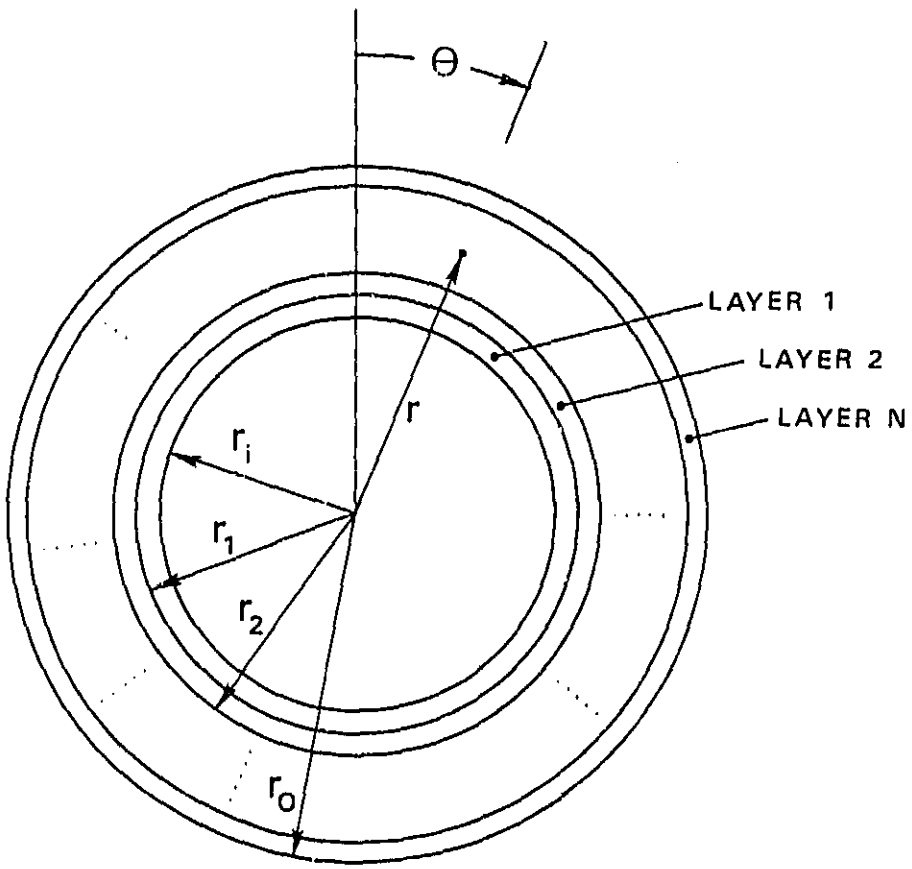

Fig. 1 Geometry and nomenclature of the tube cross-section.

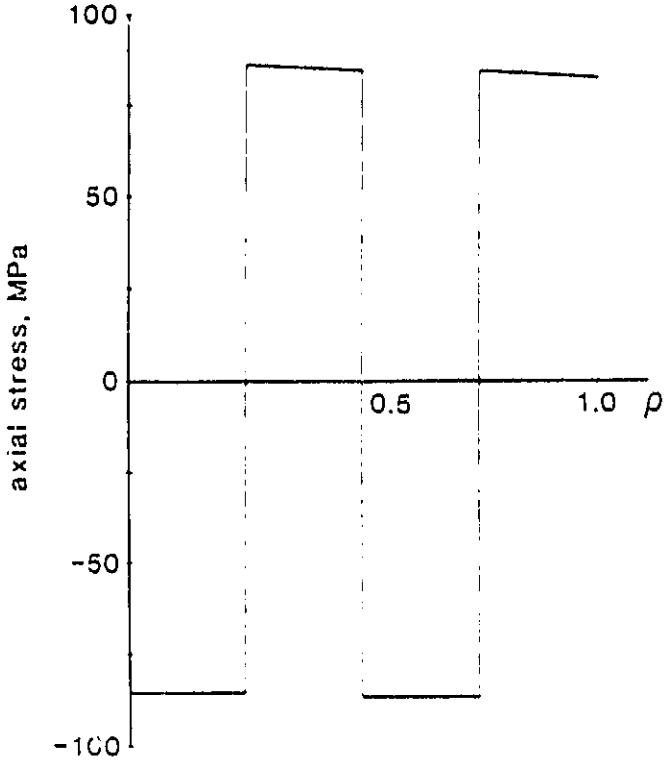

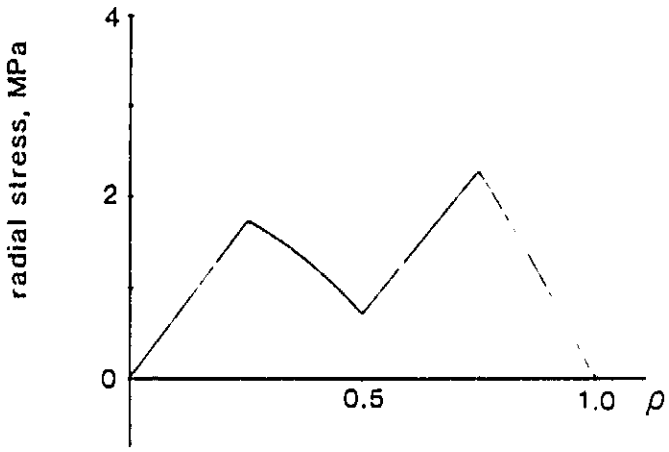

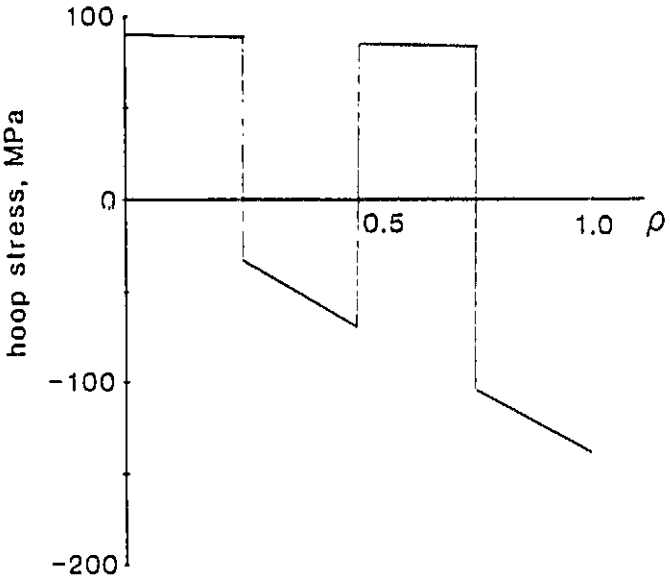

Fig. 2 Residual stresses in a (0/90/0/90) tube.

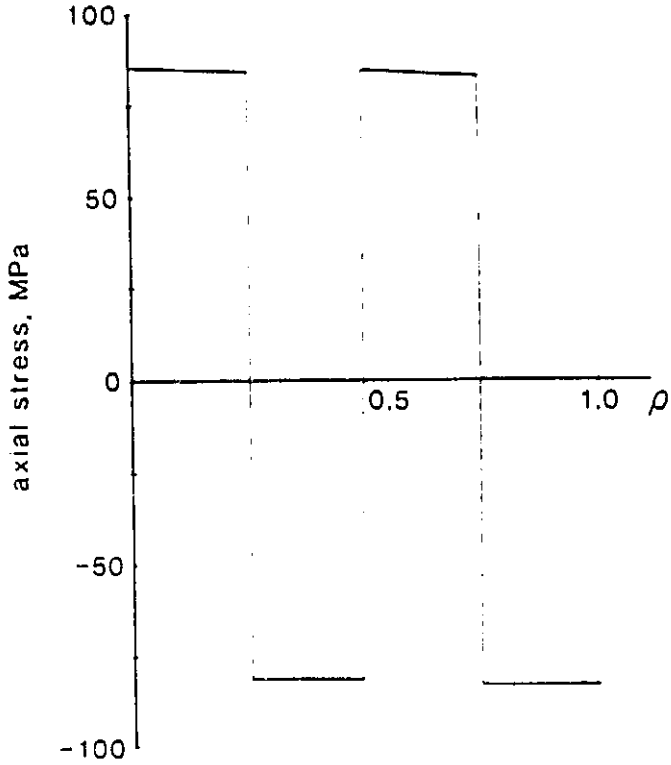

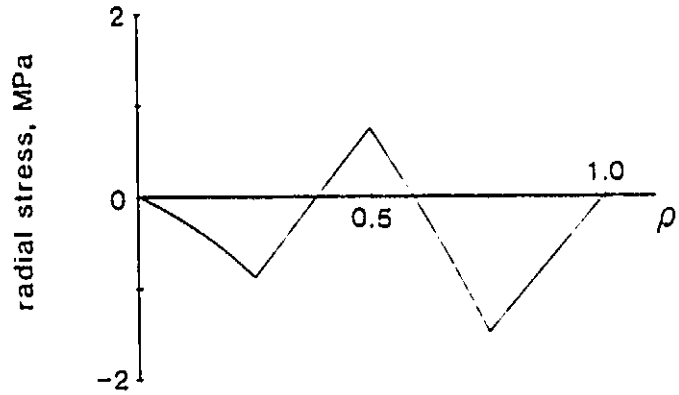

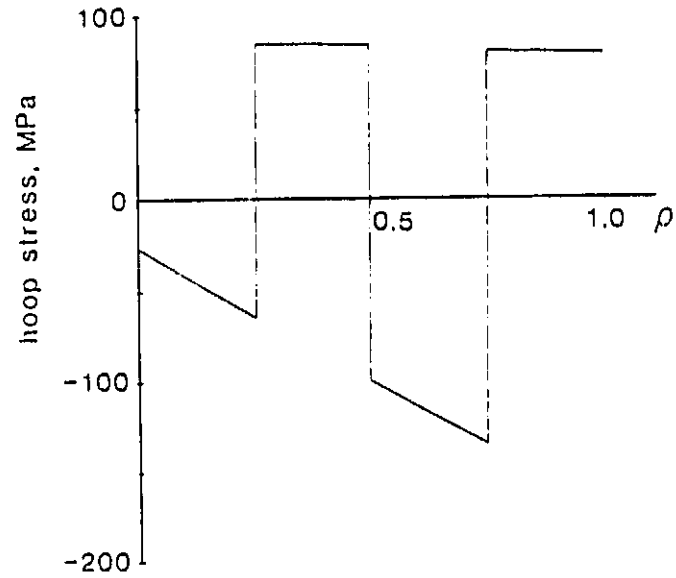

Fig. 3 Residual stresses in a (90/0/90/0) tube.

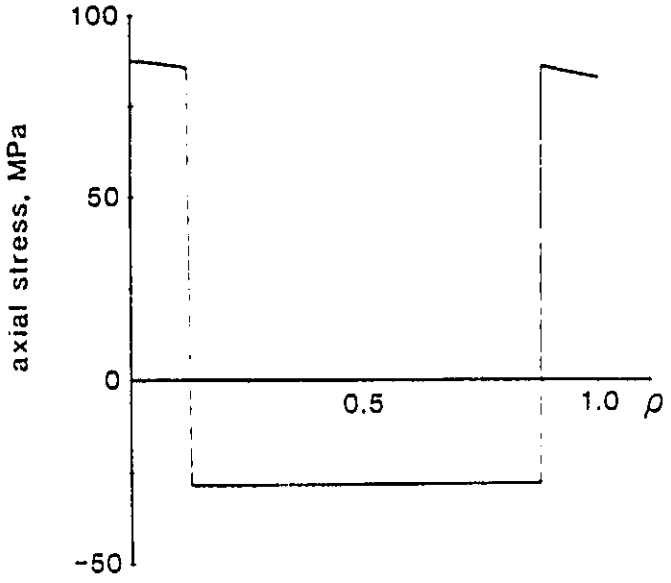

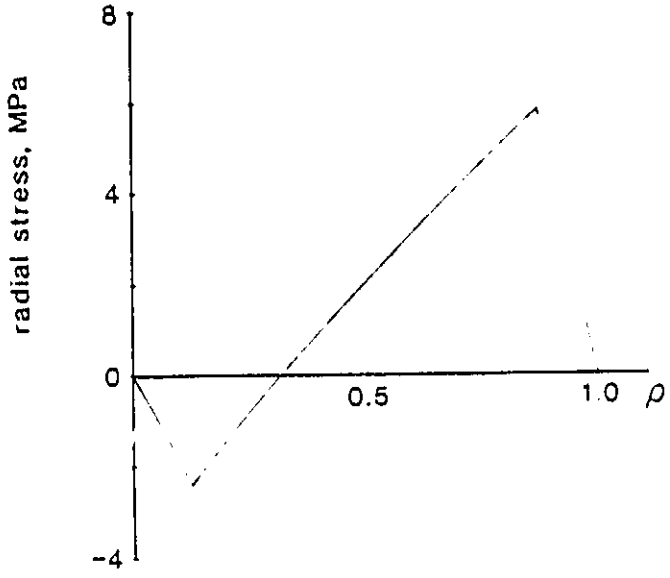

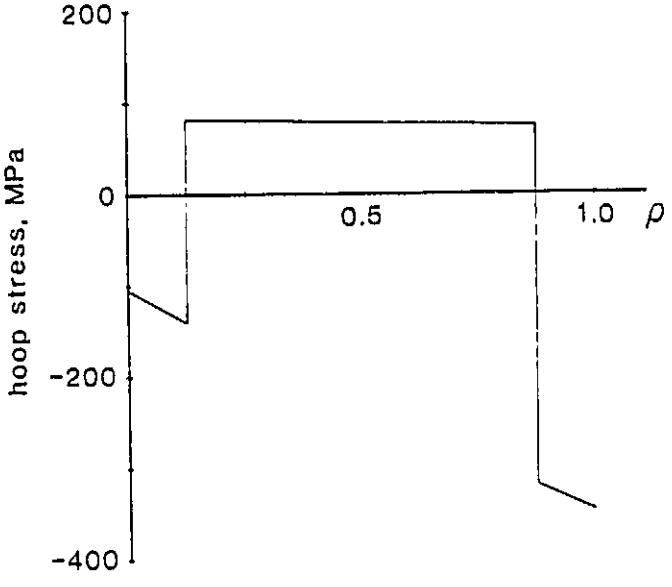

Fig. 4 Residual stresses in a $(90/0_6/90)$ tube.

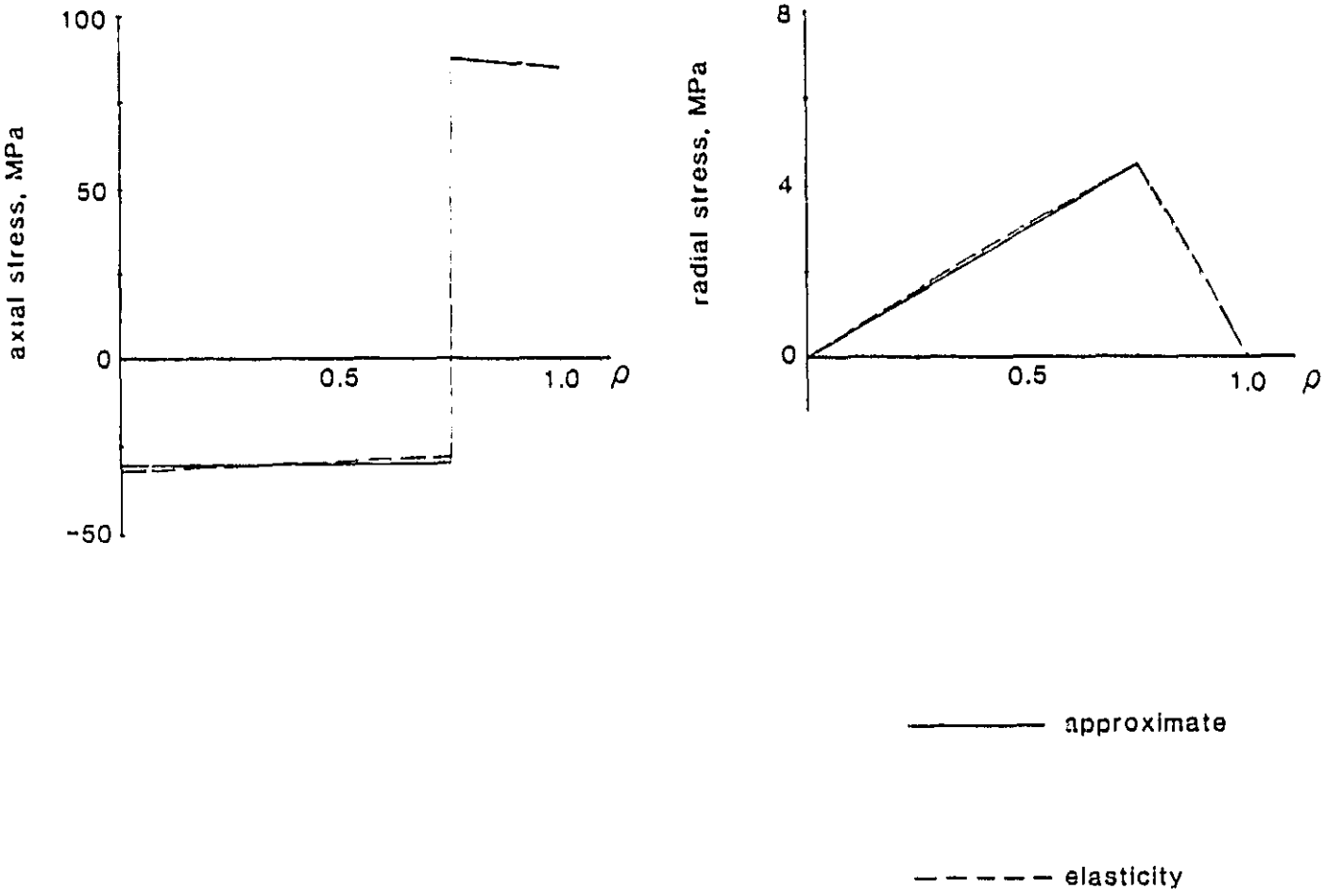

Fig. 5 Comparison between approximate and exact solutions for a $(0_3/90)$ tube.

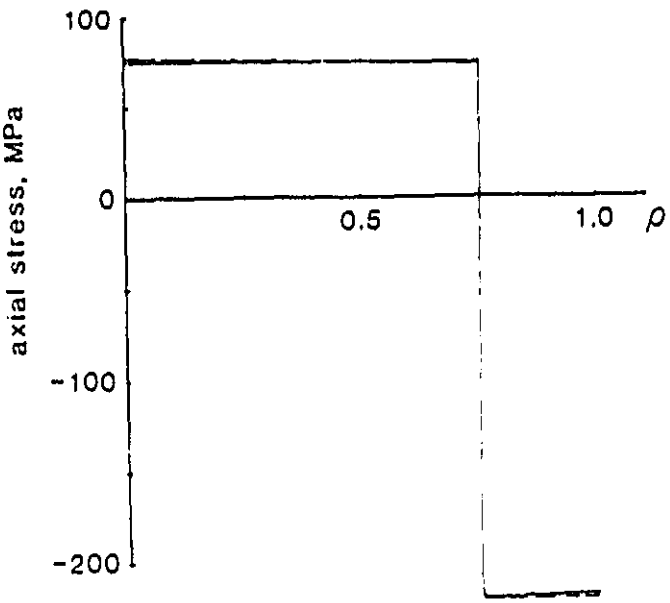

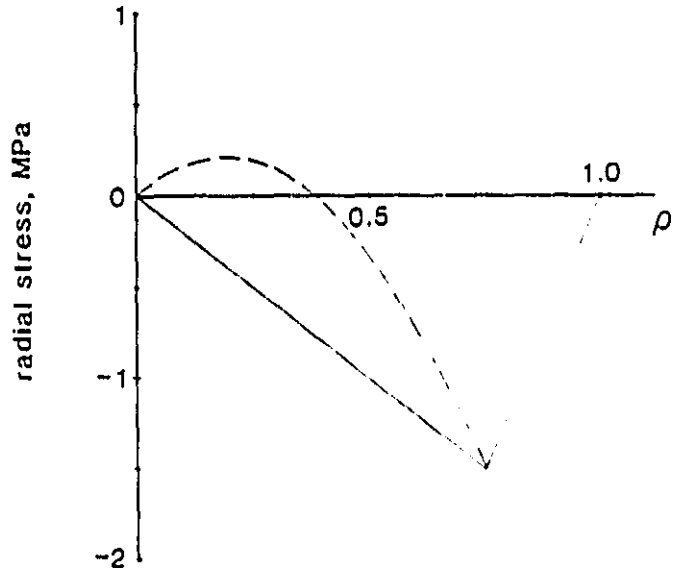

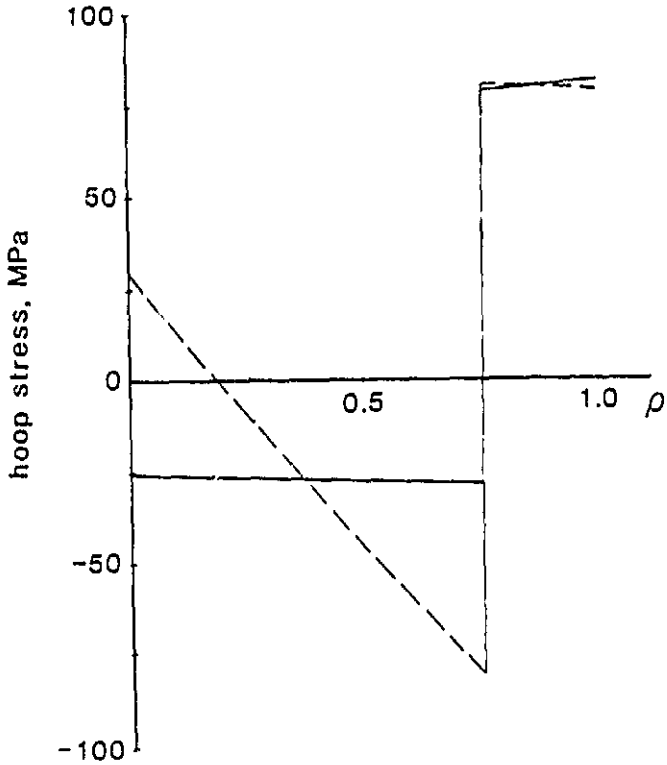

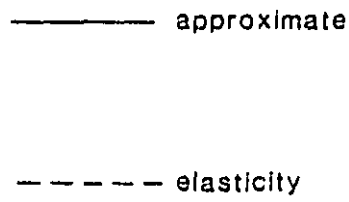

Fig. 6 Comparison between approximate and exact solutions for a $(90_3/0)$ tube.

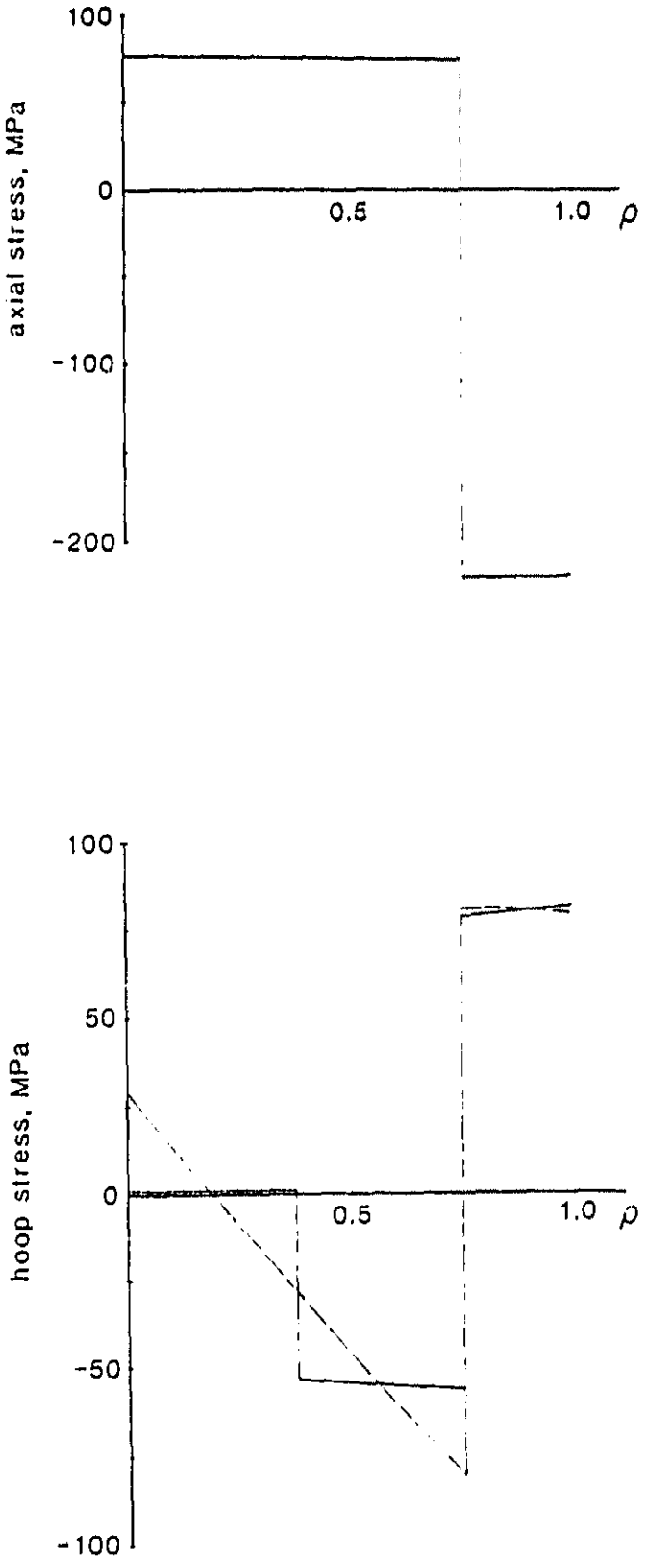

Fig. 7 Comparison between approximate and exact solutions for a $(90_3/0)$ tube, further discretization.

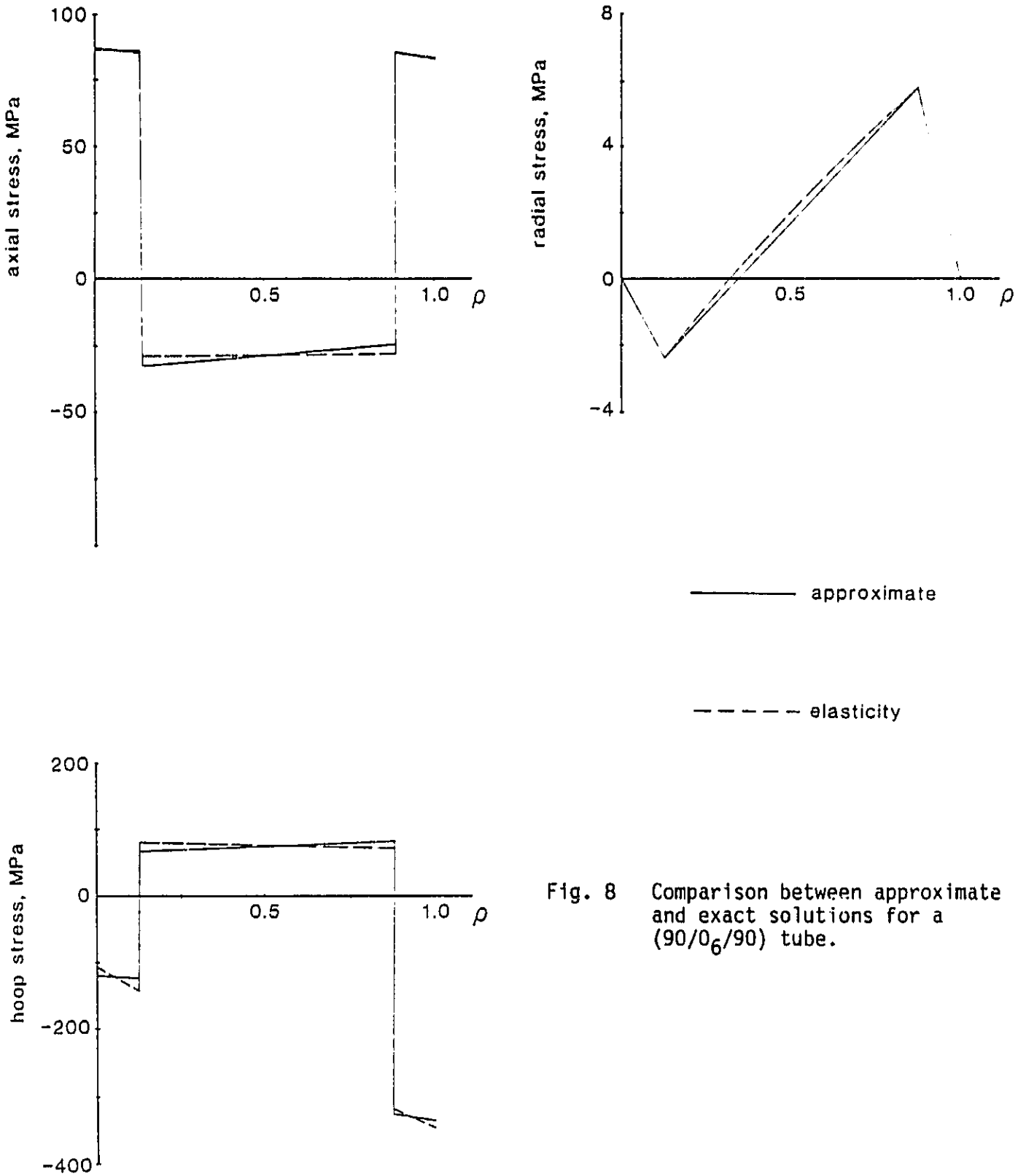

Fig. 8 Comparison between approximate and exact solutions for a $(90/0_6/90)$ tube.

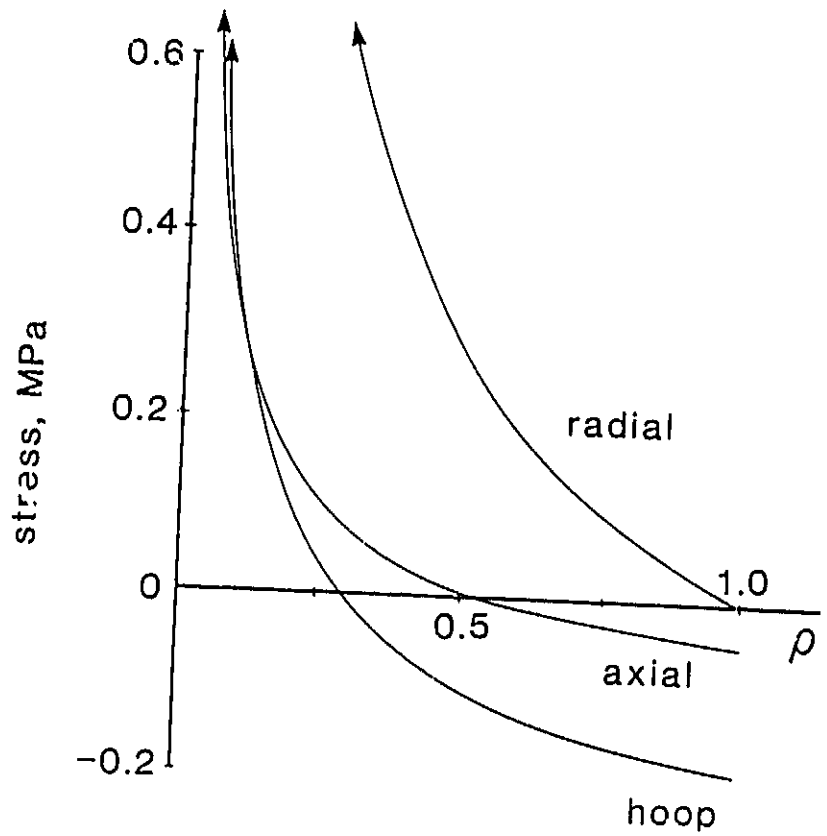

Fig. 9 Stresses in a solid cylinder $\bar{C}_{22} < \bar{C}_{33}$, $\Delta T = +1°C$.

Appendix 1

Details of the Stress-Strain Relation

Figure A1 shows a segment of a cylindrical lamina and the principal material 1-2-3 and the cylindrical x-θ-r coordinate systems. In the 1-2-3 system:

$$\begin{Bmatrix} \varepsilon_1 - \alpha_1\Delta T \\ \varepsilon_2 - \alpha_2\Delta T \\ \varepsilon_3 - \alpha_3\Delta T \\ \gamma_{23} \\ \gamma_{13} \\ \gamma_{12} \end{Bmatrix} = \begin{bmatrix} S_{11} & S_{12} & S_{13} & 0 & 0 & 0 \\ S_{12} & S_{22} & S_{23} & 0 & 0 & 0 \\ S_{13} & S_{23} & S_{33} & 0 & 0 & 0 \\ 0 & 0 & 0 & S_{44} & 0 & 0 \\ 0 & 0 & 0 & 0 & S_{55} & 0 \\ 0 & 0 & 0 & 0 & 0 & S_{66} \end{bmatrix} \begin{Bmatrix} \sigma_1 \\ \sigma_2 \\ \sigma_3 \\ \tau_{23} \\ \tau_{13} \\ \tau_{12} \end{Bmatrix} \qquad \text{(A-1)}$$

where

$$S_{11} = \frac{1}{E_1}\ ;\quad S_{12} = -\frac{\nu_{12}}{E_1}\ ;\quad S_{13} = -\frac{\nu_{13}}{E_1}$$

$$S_{22} = \frac{1}{E_2}\ ;\quad S_{23} = -\frac{\nu_{23}}{E_2}\ ;\quad S_{33} = \frac{1}{E_3} \qquad \text{(A-2)}$$

$$S_{44} = \frac{1}{G_{23}}\ ;\quad S_{55} = \frac{1}{G_{13}}\ ;\quad S_{66} = \frac{1}{G_{12}}\ .$$

The inverse of this relation is:

$$\begin{Bmatrix} \sigma_1 \\ \sigma_2 \\ \sigma_3 \\ \tau_{23} \\ \tau_{13} \\ \tau_{12} \end{Bmatrix} = \begin{bmatrix} C_{11} & C_{12} & C_{13} & 0 & 0 & 0 \\ C_{12} & C_{22} & C_{23} & 0 & 0 & 0 \\ C_{13} & C_{23} & C_{33} & 0 & 0 & 0 \\ 0 & 0 & 0 & C_{44} & 0 & 0 \\ 0 & 0 & 0 & 0 & C_{55} & 0 \\ 0 & 0 & 0 & 0 & 0 & C_{66} \end{bmatrix} \begin{Bmatrix} \varepsilon_1 - \alpha_1 \Delta T \\ \varepsilon_2 - \alpha_2 \Delta T \\ \varepsilon_3 - \alpha_3 \Delta T \\ \gamma_{23} \\ \gamma_{13} \\ \gamma_{12} \end{Bmatrix} \tag{A-3}$$

In the x-θ-r system, eq. A-1 transforms into

$$\begin{Bmatrix} \varepsilon_x - \alpha_x \Delta T \\ \varepsilon_\theta - \alpha_\theta \Delta T \\ \varepsilon_r - \alpha_r \Delta T \\ \gamma_{\theta r} \\ \gamma_{xr} \\ \gamma_{x\theta} - \alpha_{x\theta} \Delta T \end{Bmatrix} = |\bar{S}| \begin{Bmatrix} \sigma_x \\ \sigma_\theta \\ \sigma_r \\ \tau_{\theta r} \\ \tau_{xr} \\ \tau_{x\theta} \end{Bmatrix} \tag{A-4}$$

and eq. A-3 transforms into

$$\begin{Bmatrix} \sigma_x \\ \sigma_\theta \\ \sigma_r \\ \tau_{\theta r} \\ \tau_{xr} \\ \tau_{x\theta} \end{Bmatrix} = [\bar{C}] \begin{Bmatrix} \varepsilon_x - \alpha_x \Delta T \\ \varepsilon_\theta - \alpha_\theta \Delta T \\ \varepsilon_r - \alpha_r \Delta T \\ \gamma_{\theta r} \\ \gamma_{xr} \\ \gamma_{x\theta} - \alpha_{x\theta} \Delta T \end{Bmatrix} .$$

In the above

$$\bar{S}_{11} = m^4 S_{11} + m^2 n^2 (2S_{12} + S_{66}) + n^4 S_{22}$$
$$\bar{S}_{12} = \bar{S}_{21} = (m^4 + n^4) S_{12} + m^2 n^2 (S_{11} + S_{22} - S_{66})$$
$$\bar{S}_{13} = \bar{S}_{31} = (n^2 S_{23} + m^2 S_{13})$$
$$\bar{S}_{16} = mn \left[m^2 (2S_{11} - 2S_{12} - S_{66}) + n^2 (2S_{12} - 2S_{22} + S_{66}) \right]$$
$$\bar{S}_{22} = n^4 S_{11} + m^2 n^2 (2S_{12} + S_{66}) + m^4 S_{22}$$
$$\bar{S}_{23} = \bar{S}_{32} = (m^2 S_{23} + n^2 S_{13})$$
$$\bar{S}_{26} = mn \left[m^2 (2S_{12} - 2S_{22} + S_{66}) + n^2 (2S_{11} - 2S_{12} - S_{66}) \right]$$
$$\bar{S}_{33} = S_{33}$$
$$\bar{S}_{36} = \bar{S}_{63} = 2mn(S_{13} - S_{23})$$
$$\bar{S}_{44} = m^2 S_{44} + n^2 S_{55}$$
$$\bar{S}_{45} = \bar{S}_{54} = mn(S_{55} - S_{44})$$
$$\bar{S}_{55} = n^2 S_{44} + m^2 S_{55}$$
$$\bar{S}_{66} = 4m^2 n^2 (S_{11} - 2S_{12} + S_{22}) + S_{66} (m^2 - n^2)^2$$

$$m = \cos\phi \qquad n = \sin\phi \quad .$$

Also

$$\alpha_x = m^2\alpha_1 + n^2\alpha_2; \quad \alpha_\theta = n^2\alpha_1 + m^2\alpha_2, \; \alpha_r = \alpha_3$$

$$\alpha_{\theta r} = 0 = \alpha_{xr}; \quad \alpha_{x\theta} = 2mn(\alpha_1 - \alpha_2) \; ,$$

and

$$\begin{aligned}
\bar{C}_{11} &= m^4C_{11} + 2m^2n^2(C_{12} + 2C_{66}) + n^4C_{22} \\
\bar{C}_{12} &= n^2m^2(C_{11} + C_{22} - 4C_{66}) + (n^4 + m^4)C_{12} \\
\bar{C}_{13} &= m^2C_{13} + n^2C_{23} \\
\bar{C}_{16} &= mn[m^2(C_{11} - C_{12} - 2C_{66}) + n^2(C_{12} - C_{22} + 2C_{66})] \\
\bar{C}_{22} &= n^4C_{11} + 2n^2m^2(C_{12} + 2C_{66}) + m^4C_{22} \\
\bar{C}_{23} &= n^2C_{13} + m^2C_{23} \\
\bar{C}_{26} &= mn[n^2(C_{11} - C_{12} - 2C_{66}) + m^2(C_{12} - C_{22} + 2C_{66})] \\
\bar{C}_{33} &= C_{33} \\
\bar{C}_{36} &= mn(C_{13} - C_{23}) \\
\bar{C}_{44} &= m^2C_{44} + n^2C_{55} \\
\bar{C}_{45} &= mn(C_{55} - C_{44}) \\
\bar{C}_{55} &= n^2C_{44} + m^2C_{55} \\
\bar{C}_{66} &= m^2n^2(C_{11} - 2C_{12} + C_{22}) + C_{66}(m^2 - n^2)^2 \quad .
\end{aligned}$$

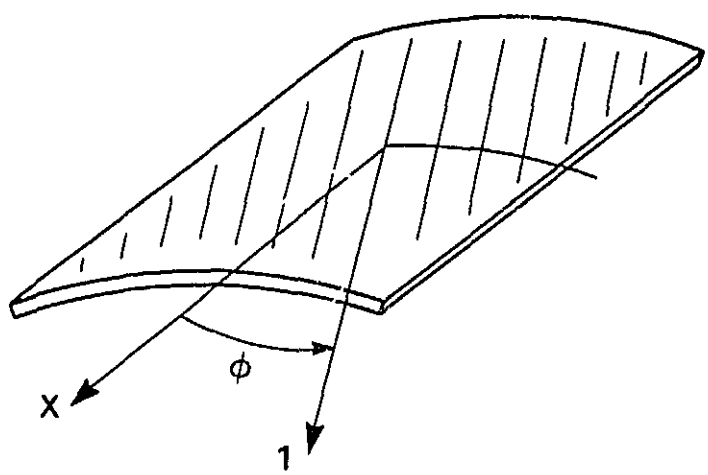

Fig. A-1 Segment of cylindrical lamina.

Appendix 2

Definition of Constants in Approximate Method

$$\beta_1 = F_2/H_2; \quad \beta_2 = H_1/H_2; \quad \beta_3 = G_2/H_2$$

$$F_2 = (r_1^3 - r_i^3)/3; \quad H_1 = (r_1^2 - r_i^2)/2; \quad G_2 = (r_o^3 - r_1^3)/3$$

$$H_2 = (r_o^2 - r_1^2)/2 \quad .$$

r_i = inner tube radius

r_o = inner tube radius

r_1 = radius to interface between layers.

1 Report No	2 Government Accession No	3 Recipient's Catalog No
CCMS-85-06, VPI-E-85-15		

4 Title and Subtitle
Stresses and Deformations in Cross-Ply Composite Tubes Subjected to a Uniform Temperature Change: Elasticity and Approximate Solutions

5 Report Date
June 1985

6 Performing Organization Code

7 Author(s)
M. W. Hyer, David E. Cooper, D. Cohen

8 Performing Organization Report No.
CCMS-85-06
VPI-E-85-15

9 Performing Organization Name and Address
Department of Engineering Science and Mechanics
Virginia Polytechnic Institute & State University
Blacksburg, VA 24061-4899

10 Work Unit No.

11 Contract or Grant No
NAG-1-343

12 Sponsoring Agency Name and Address
National Aeronautics and Space Administration
Langley Research Center
Hampton, VA 23665

13 Type of Report and Period Covered
Interim 6/84 - 6/85

14 Sponsoring Agency Code

15 Supplementary Notes

16 Abstract

The study: (1) Investigates the effects of a uniform temperature change on the stresses and deformations of composite tubes; (2) Determines the accuracy of an approximate solution based on the principle of complementary virtual work. Interest centers on tube response away from the ends and so a planar elasticity approach is used. For the approximate solution a piecewise linear variation of stresses with the radial coordinate is assumed. The results from the approximate solution are compared with the elasticity solution. The stress predictions agree well, particularly peak interlaminar stresses. Suprisingly, the axial deformations also agree well. This despite the fact that the deformations predicted by the approximate solution do not satisfy the interface displacement continuity conditions required by the elasticity solution. The study shows that the axial thermal expansion coefficient of tubes with a specific number of axial and circumferential layers depends on the stacking sequence. This is in contrast to classical lamination theory which predicts the expansion to be independent of the stacking arrangement. As expected, the sign and magnitude of the peak interlaminar stresses depends on stacking sequence. For tubes with a specific number of axial and circumferential layers, thermally-induced interlaminar stresses can be controlled by altering stacking arrangement.

17 Key Words (Suggested by Author(s))	18. Distribution Statement
cross-ply tubes, residual stresses, coefficient of thermal expansion, principle of complementary virtual work, approximate methods	unlimited

19 Security Classif. (of this report)	20. Security Classif. (of this page)	21. No. of Pages	22. Price
unclassified	unclassified	48	